

Article

Research on Seismic Performance of Frame Structure with Beam Staircases

Ming Wen, Hongxiang Tian, Weiwei Wang, Baokui Chen * and Huayao Fu

School of Infrastructure Engineering, Nanchang University, Nanchang 330031, China; wenming@ncu.edu.cn (M.W.); 401127020011@email.ncu.edu.cn (H.T.); 401127020005@ncu.edu.cn (W.W.); 411115620011@email.ncu.edu.cn (H.F.)

* Correspondence: bkchen@ncu.edu.cn

Abstract: Beam staircases are widely used in frame structures. In structural design, stair flights are often ignored in the model establishment, and their loads are only added to the stair beams. However, under a seismic load, the flight of stairs will increase the staircase's stiffness and affect the seismic response characteristics of the stairs and even of the structure. According to the engineering example, the finite element numerical models of the pure frame structure without staircases, the frame structure with fixed connection beam staircases, and the frame structure with sliding connection beam staircases were established. Modal analysis, response spectrum analysis, and elastic time-history analysis were carried out. By comparing the maximum story displacement, story displacement angle, natural period, story shear force, and the internal force of components of each model, the influences of beam staircases and their bearing connection mode on the seismic performance of the building were analyzed. In addition, by examining the frame model with sliding connection beam stairs, the influences of different staircase positions on the seismic performance of the building were studied. Finally, the advantages and disadvantages of different design schemes were compared, and the effects of the modeling method, support type, and layout position of the beam staircases on the seismic performance of the frame structure were summarized. The conclusions are that the story drift angle of the sliding connection structure is larger than that of the fixed connection structure, and the internal force of the frame columns of the former is smaller than that of the latter. Moreover, the positions of the staircase will affect the horizontal displacement of the structure.

Keywords: beam staircase; sliding bearing; numerical simulation; seismic performance



Citation: Wen, M.; Tian, H.; Wang, W.; Chen, B.; Fu, H. Research on Seismic Performance of Frame Structure with Beam Staircases. *Buildings* **2022**, *12*, 1106. <https://doi.org/10.3390/buildings12081106>

Academic Editors: Chunxu Qu, Shibin Lin, Donghui Yang and Sadegh Shams

Received: 30 June 2022

Accepted: 23 July 2022

Published: 27 July 2022

Publisher's Note: MDPI stays neutral with regard to jurisdictional claims in published maps and institutional affiliations.



Copyright: © 2022 by the authors. Licensee MDPI, Basel, Switzerland. This article is an open access article distributed under the terms and conditions of the Creative Commons Attribution (CC BY) license (<https://creativecommons.org/licenses/by/4.0/>).

1. Introduction

Many investigations and studies have shown that earthquakes inflict substantial damage on staircases and even cause some to collapse [1,2]. Although stairs make it possible for people to escape a building during an earthquake, they often hinder the rescue work afterward. However, in most structural calculations, the stairs and the structure are not considered as a whole; the stair design is usually considered separately from the main structure. In stair design, only the vertical load is considered; neither the impact of the earthquake nor the interaction between the main structure and the staircase are considered; it ignores the axial tension and compression force on the stair board during the earthquake. Therefore, it is necessary to strengthen the research on stair components to improve the seismic performance of buildings and reduce the harm to life and property caused by earthquakes.

There is a large body of research on the seismic performance of stair structures. Cosenza et al. [3] conducted static elastic–plastic analysis of two stairs and obtained the typical failure modes of the stair components under the bending moment and shear force. The results showed that the presence of stairs can improve the stiffness and strength of a structure. Bilal et al. [4] studied the effect of stairs on the buildings' seismic performance.

When stairs are factored into the seismic analysis, the natural vibration period of the building will be significantly shortened. At the same time, the best location for stairs is in the middle bay of the building where there is less attraction of shear force than on the end. Cong et al. [5] used a reinforced concrete frame to support the floor around the stairs with separate slabs near the frame columns. This case prevented the shear failure of the building columns around the stairs and achieved 53.46% greater lateral stiffness than the ordinary frame model. Liu et al. [6] used ETABS to study the impact of sliding bearing stairs on the structure's seismic performance after the release of diagonal bracing and found that sliding bearing could reduce the lateral stiffness of the building and the effects of seismic damage. Ma [7] used ANSYS to study the influence of different forms of stairs on the seismic performance of the building and concluded that stairs could significantly increase the structural stiffness. According to their experimental results, Wu et al. [8] established a relationship between the story drift angle and the seismic performance of the stair unit; they used these findings to propose a method of evaluating the seismic performance of the slab stair. Fallahi et al. [9] conducted a pushover analysis on the RC frame and considered whether or not stairs were involved in modeling, the location of stairs, and whether or not the building plane is irregular when assessing the seismic performance of a structure. Ahmad [10] established the stiffness matrix according to the geometric parameters of unsupported stairs and calculated the internal forces of each component. The results showed that the lateral stiffness of the stairs has a greater impact on the structure, and is affected by shear deformation. Kam [11] found that a high-rise building collapsed from earthquake damage to the prefabricated staircase connection. Wang et al. [12] used findings from a shake-table experiment to find that most structural damage occurred at the connection of stairs, where there is insufficient strength. They also found that stair connections are easily damaged by repeated tension and compression during an earthquake.

Karaaslan et al. [13] examined the influence of staircases on the seismic response of substandard RC frame buildings, which differed in the number of stories and spans, the presence and position of staircases, and the conducted modal analyses and bi-directional nonlinear time history analyses. Feng et al. [14] conducted elastic analyses for 18 RC structure models with and without staircases to study the influence of the staircase on the stiffness, displacement, and internal forces of the structures. Khadse et al. [15] conducted a comparative analysis of the G+10 RC building staircase model at different locations; they found that the presence of a staircase had a tremendous influence on the design of the beam and column on the periphery of the staircase. Zhao et al. [16] conducted a shake-table test on a concrete frame staircase with sliding bearings. Their test results showed that the structural unit of the stair with sliding support at the bottom of the staircase slab had good seismic behavior, and the damage was concentrated in the frame beams and columns of the staircase. Ke et al. [17] proposed an earthquake-resistant frame staircase model with damped bearings and performed a finite element analysis of a nine-story reinforced concrete structure using SAP2000. They concluded that the improved viscous damping bearing model could change the uneven distribution of the structure's stiffness caused by the stairs and improve its ductility.

In addition, the existence of a staircase can produce high torsional eccentricities and attract large seismic loads, leading to the failure of supporting elements such as columns and landing beams. At the same time, a horizontal bracing effect is developed by the existence of a staircase, leading to a decrease in the vibration period and inter-story displacement where the greater the bracing effect, the more changes there are in the distribution of straining actions [18]. When stairs are factored into the analysis, the presence of stairs increases the maximum lateral shear force of the building, leading to column failure when both its flexural and shear hinges reach a stage of collapse [19]. However, the bracing effect of stairs will improve the performance of the structure during the earthquake and increase the stiffness of the building [20]. The slab-bearing stairs were tested under cyclic loading, and the failure modes of the stair components were similar to those in earthquakes [21,22]. According to the finite element analysis of two six-story buildings, it can be found that

the stairs have minimal influence on the dynamic characteristics of the structures [23]. Considering that the staircases in the calculation will increase the structure's stiffness and reduce the story displacement, and the change in the location of staircase has a significant impact on the force of the frame column [24].

The above research on the seismic performance of stair structures shows that most scholars or institutions have mainly studied the cast-in-place slab stairs or fabricated stairs in the seismic analysis of stairs. There are few studies on the seismic performance of beam staircases, and the factors that affect the performance of the stairs have been even less considered, there is lack of systematic consideration of the influences of various factors and comprehensive research on the performance of reinforced concrete stairs. In addition, in most cases, the stairs were not factored into the structural seismic analysis. There have been few reports on the seismic performance of the frame structure with the sliding connection of beam staircases, and the failure process and mode are still unclear.

In this work, we simulated the seismic performance of the frame structure with beam staircases and considered the stiffness of the stairs and the interaction between the stairs and the structure to analyze its performance and safety during earthquakes. We then compared the seismic performance of the beam staircases under different bearing connection modes. Through modal analysis, response spectrum analysis, and elastic time history analysis, this study makes up for the insufficient research on the seismic performance of frame structures with beam staircases under different forms of support. This study offers a new data reference for the practical application of beam staircases and has practical significance for building engineers.

2. Numerical Model and Verification

2.1. Model Information

To verify the accuracy of the FEA software used in this paper, this section presents three single-story frame models. Model A is a pure frame with no stairs, model B is a fixed joint stairwell model, and model C is a sliding bearing stairwell model. ABAQUS and ETABS were used to carry out the modal analysis and static pushover analysis on each model. We then compared the results and verified the accuracy of the results.

The dimensions of the three types of stairwells were the same: the floor height was 4 m, the staircase was 4.3 m wide and 6.4 m deep, and the staircase slab was 2 m wide. The frame column was 450 mm × 450 mm, the frame beam was 250 mm × 600 mm, the landing slab was 100 mm thick, the stair beam was 200 mm × 400 mm, and the stair column was 250 mm × 250 mm. The stairwell was made of C30 concrete (the compressive strength is 30 MPa). The reinforcement was HRB400 grade steel (the yield strength is 400 N/mm²). Because the type of stairs analyzed in this paper is the most common in China, structural reinforcement was carried out according to Chinese Code 11 G101-2 [25]. The seismic intensity was 7 degrees, the seismic grouping was one group, and the site category was Class II. Figure 1 shows the structure and modeling method of the sliding bearing. Because of the large seismic force, the model did not consider the influence of the contact friction of the sliding bearing.

When using ABAQUS software for modeling the calculation, no stair steps are built in the model because the steps participate in the load transfer but not in the structural stress. It is therefore difficult to obtain high-quality mesh division during model meshing. The concrete model adopted the plastic damage model, and the reinforcement model was the bilinear model, embedded in the concrete element using built-in regions. The "Tie" was used to simulate the fixed connection between the stair beams and the landing slabs. Interactions were used to simulate the sliding connections; when setting the interaction property, the property of tangential contact was set to frictionless and the property of normal contact to hard contact. The built-in area in the constraint manager was used to simulate the interaction between the reinforcement and concrete frame. The selected type of concrete was an eight-node linear hexahedron reduced integration element (C3D8R),

and the reinforcement was the 2-node 3-dimensional truss element (T3D2). The models are in Figure 2.

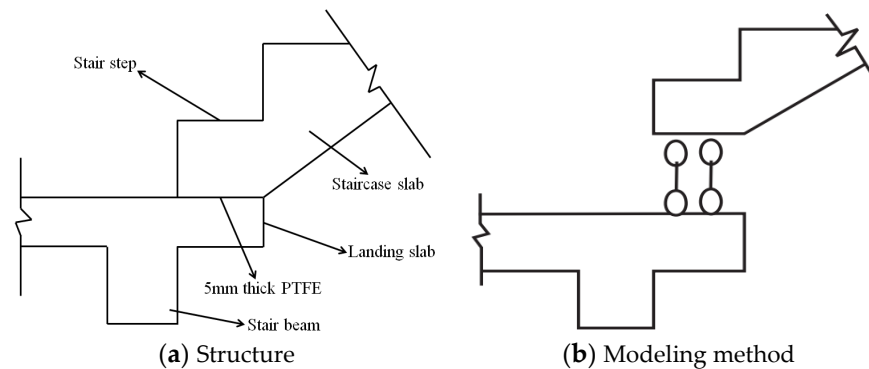


Figure 1. Structure and modeling method of the sliding bearing.

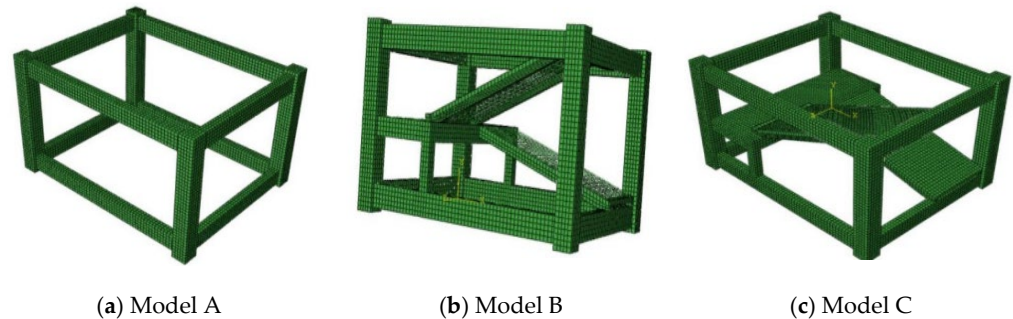


Figure 2. The ABAQUS models.

When using ETABS for structural modeling, we used the membrane elements to simulate the floor, and the assumption of a rigid diaphragm to ensure the floor's infinite rigidity. We used the 100 mm thick shell elements to simulate the staircase slab and the bar elements to simulate the frame beams, frame columns, stair beams, stair columns, and inclined beams. The fixed connection between the bottom of the model and the foundation was realized by constraining the translational and rotational degrees of freedom in three directions at the bottom of the model.

Elastic rods and default plastic hinges were used to simulate the beams and columns. Bending hinges M3 were considered for the beams, PMM hinges for the columns, and PMM hinges and shear hinges V2 for the bottom columns. Plastic hinges were placed at the ends of the rods; at the connection between frame columns, and landing slabs PMM and V2 hinges were set up. M3 and V2 hinges were installed at the end and middle parts of the stair beams. The stair columns were installed with PMM and V2 hinges. The models are shown in Figure 3.

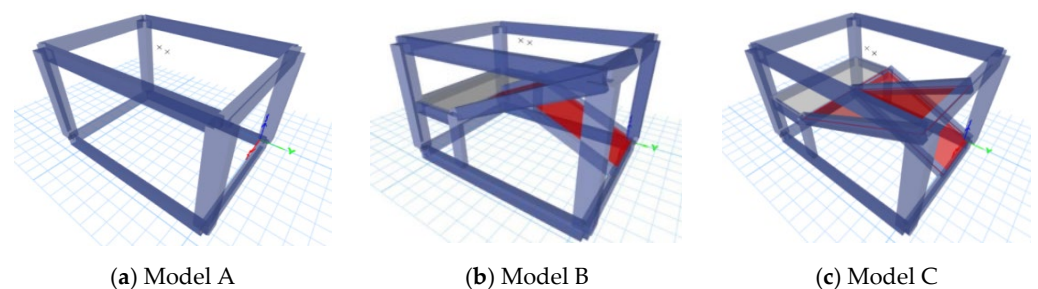


Figure 3. The ETABS models.

2.2. Model Verification

2.2.1. Modal Analysis

Table 1 presents the results of the comparison of the self-oscillation periods of the first three-order cycles of the extracted models.

Table 1. A comparison of the natural frequency of the models.

Model	Vibration Mode	ABAQUS	ETABS	ABA-ETA/ABA
Model A	Vibration type 1	5.79	5.52	4.66%
	Vibration type 2	6.59	6.14	6.83%
	Vibration type 3	6.54	6.21	5.05%
Model B	Vibration type 1	10.49	9.85	6.10%
	Vibration type 2	15.68	14.72	6.12%
	Vibration type 3	18.96	18.22	3.90%
Model C	Vibration type 1	4.85	4.70	3.10%
	Vibration type 2	6.00	5.75	4.17%
	Vibration type 3	6.70	6.36	5.07%

According to the modal analysis, the results obtained by the ABAQUS and ETABS simulations were similar, the difference in the self-oscillation frequencies of the first three-orders of vibration was low, and the errors were less than 10%, meeting the accuracy requirements of the simulation.

2.2.2. Static Pushover Analysis

When using ABAQUS to carry out the static pushover analysis, three analysis steps are set. The gravity load, the vertical concentrated force, and the horizontal pushover force are applied, respectively, by using the inverted triangle node loading mode, and the vertical concentrated force is the equivalent concentrated force of the total load. The loading mode of ETABS is also an inverted triangle loading mode. The relationships between the base shear force and the vertex displacement of each model were compared, and the results are shown in Figure 4.

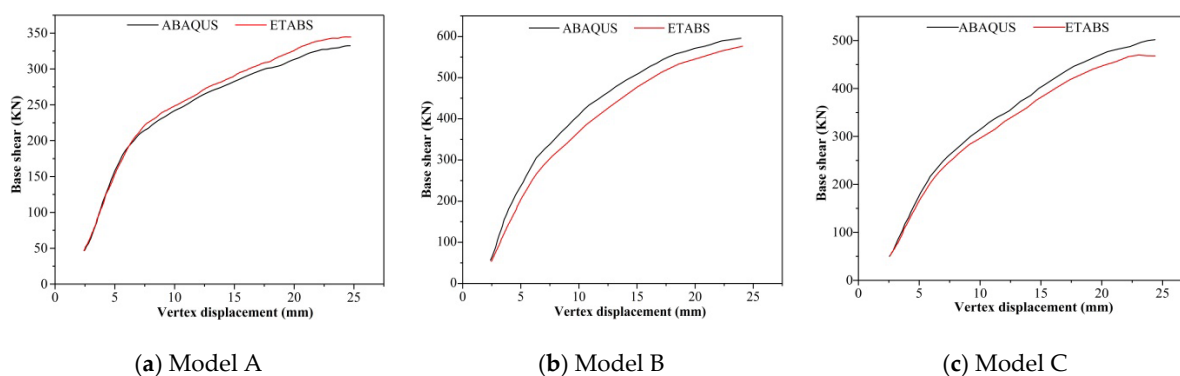


Figure 4. The base shear–vertex displacement curves.

As can be seen from the graphs, the curves derived from the two software programs overlapped considerably. The declines in stiffness were almost identical. The maximum difference between the two curves was 9.57%, which was less than 10%, so the results simulated by the two software programs were similar, the steps taken to model the analysis are reasonable, and the results are highly credible. The simulation results were consistent with experimental results [16].

3. Engineering Project and Modeling Approach

3.1. Different Bearing Designs

To study the difference in the seismic performance of the frame model without the staircases, the frame model with fixed connection beam staircases, and the frame structure model with sliding connection beam staircases, this paper selected a six-story pure frame structure teaching building as the research object. Each story is 4 m high. There are three transverse spans: 6.2 m, 2.5 m, and 6.2 m. There are eight 4.6 m spans in the longitudinal direction. The frame columns are 400 mm × 500 mm and the frame beams are 300 mm × 500 mm. The standard floor slabs are 100 mm thick. Each stair step is 130 mm × 270 mm, the stairwell is 600 mm wide, the staircase slab is 4050 mm long and 2000 mm wide, and rest of the platform is 2000 mm wide. The landing slab and staircase slab are 100 mm thick. The columns, beams, slabs, and stair members are all made of C30 concrete (the compressive strength is 30 MPa), and the longitudinal reinforcement of the beams and columns is HRB400 steel (the yield strength is 400 MPa). The longitudinal reinforcement used in the beams and columns is HRB400 reinforcement, and the hoop reinforcement is HPB235 reinforcement (the yield strength is 235 MPa). The basic wind pressure of the building is 0.35, the ground roughness is C, the seismic intensity is 7 degrees, the seismic grouping is one group, and the site category is Class II.

When ETABS is used to model the structure of each model, the method remains unchanged. The floor is still assumed to be a rigid diaphragm, and the frame beams and columns are still stimulated by spatial bar elements [26]. Our three models were as follows:

Model D: No staircases in the stairwell, and the stairs were not factored into the overall calculation.

Model E: A beam staircase is in the stairwell, and the staircase bearing connection was the fixed connection.

Model F: A beam staircase with a fixed connection for the upper support and a sliding connection for the lower is in the stairwell. The three completed models are shown in Figure 5.

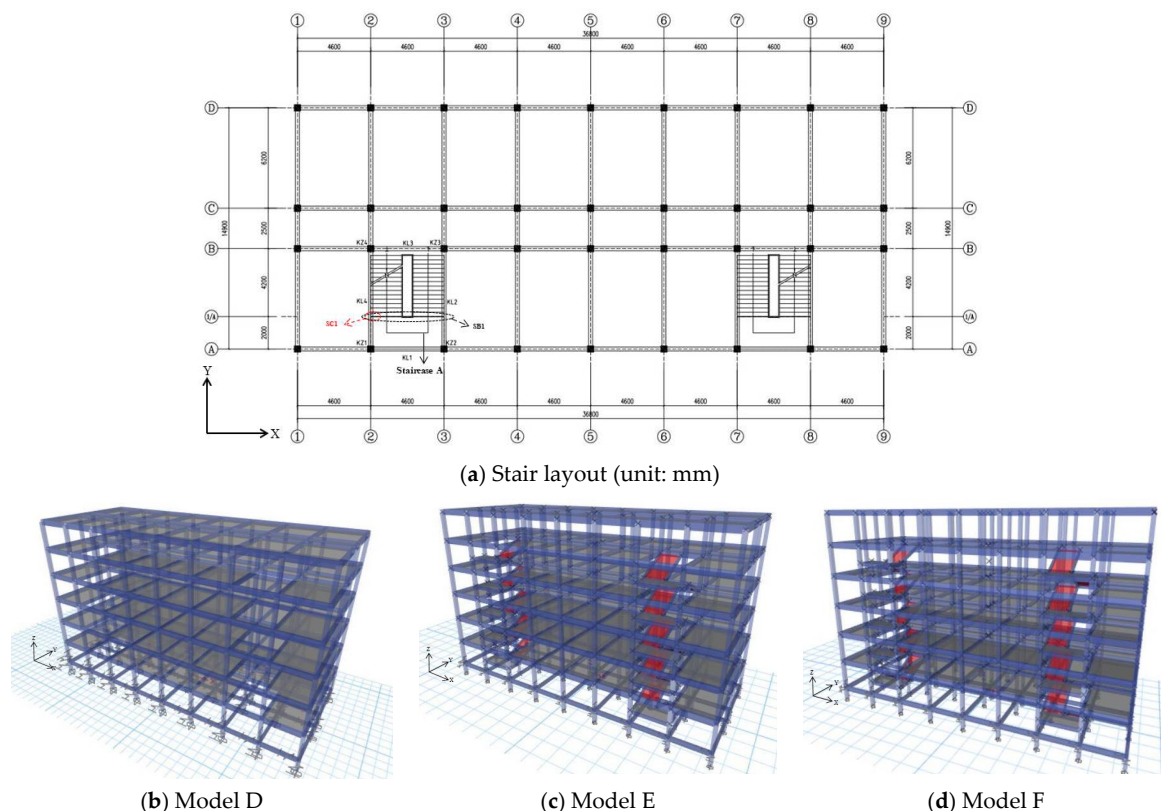


Figure 5. The three ETABS models.

3.2. Different Staircase Positions

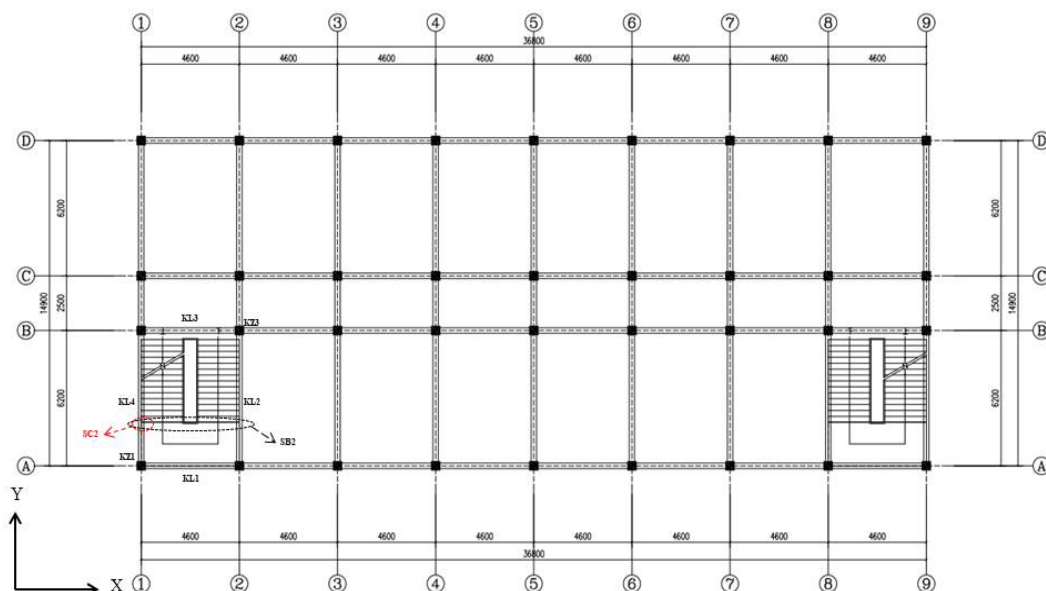
After the sliding connection bearing is installed, the seismic action of the main structures and the damage to the stair components will be reduced. This improves the seismic performance of the building, reduces the damage to people and property, and is consistent with the needs of the project. This section examines the change in the structural seismic performance under different stair arrangements following changes in the position of the sliding connection beam staircases.

Model F is a six-story frame structure with sliding connecting beam staircases. Parameters such as structural information and working condition settings were unchanged, model G and model H had stairs in different locations.

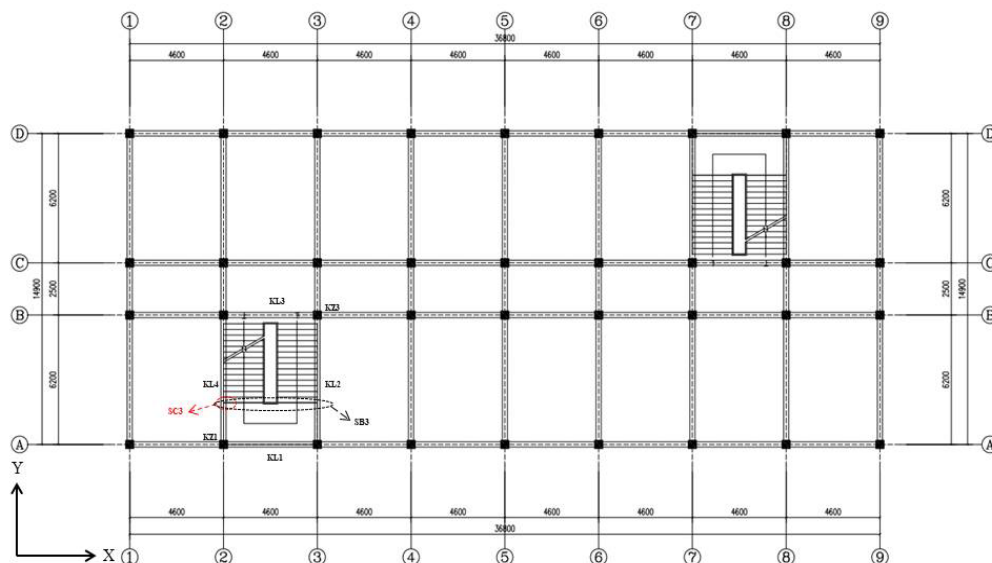
Model G: The stairs in model F were moved outward one span in the longitudinal direction and placed on the side span.

Model H: The stairs in model F were moved into a symmetrical position according to the center of the plane.

Figure 6 shows the plane layouts of model G and model H.



(a) Model G (unit: mm)



(b) Model H (unit: mm)

Figure 6. The layout plan of the models.

The frame structure used in the simulation is rather common, and its plane layout is uniform, meeting the design requirements of daily engineering. The design of the location and size of the stairs meet the specifications and the layout form reflects the layout of the project. The models after ETABS modeling are shown in Figure 7.

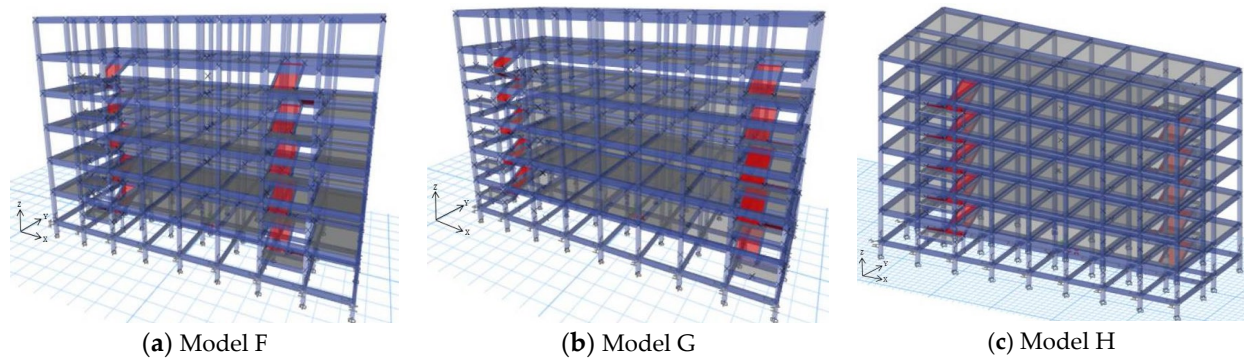


Figure 7. The models of three different staircase positions.

4. Numerical Results

4.1. Different Bearing Designs

4.1.1. Modal Analysis

Modal analysis is the most commonly used and effective method in the seismic analysis of linear structures. It is also the basis of dynamic analysis such as response spectrum and time history analysis, which can provide a reference for the static analysis of structures. In the modal analysis of the three models, the first 12 vibration modes were compared to study the influence of different stair settings on the natural vibration period of the structure. The comparison of the first 12 natural vibration periods is shown in Figure 8, and the comparison of the direction of the first three vibration modes is presented in Table 2.

In Figure 8, the values of the first three-order vibration periods were larger. From the fourth-order vibration period, the period of each model decreased sharply. The decrease in the natural period of model D was larger than that of the other two models. The decrease rate of each model in the later period was more moderate, indicating that the natural period of the structure was determined mainly by the first three-orders of vibration. The overall trend also showed that the order of the natural period of the three models from largest to smallest was model D > model F > model E.

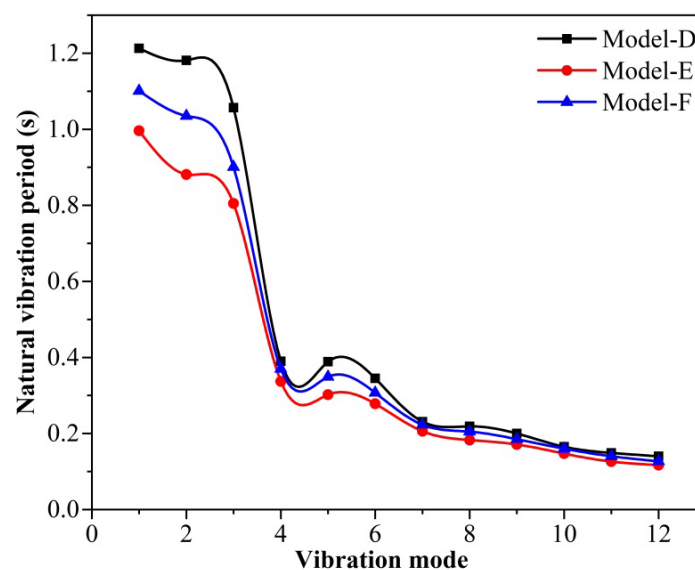


Figure 8. A comparison of the model's natural period.

The first three-orders of the natural period of model D were larger than model E, which indicates that the structure's stiffness will be reduced, and the natural period will increase if the staircases are not factored into the modeling. The natural period of model F was larger than model E and smaller than model D, which indicates that the lateral and torsional stiffness of the staircase with a sliding connection is smaller than the fixed connection, and the staircase's influence on the dynamic characteristics of the structure is reduced. Although the sliding bearing can reduce the deformation constraint between the stair beam and the landing slab, the staircase still increases the stiffness. This influencing factor needs to be considered in the seismic design.

From Table 2, we know that when excluding the stairs from the modeling calculation, the first two vibration modes of the structure are the Y-direction and X-direction translation. Otherwise, the first two vibration modes of the building are changed to the X-direction and Y-direction translation. In other words, the stairs will affect the order of the appearance of the structural modes when they are in the structural calculation.

Table 2. The direction of the vibration mode of models.

Vibration Model	Model D	Model E	Model F
1	Y-translation	X-translation	X-translation
2	X-translation	Y-translation	Y-translation
3	Z-torsion	Z-torsion	Z-torsion

4.1.2. Response Spectrum Analysis

(1) Maximum horizontal displacement

The maximum elastic inter-story drift should meet the requirements of the code when checking the seismic deformation of the structure following frequent earthquakes. For reinforced concrete frame structures, the limit value of the inter-story drift angle is $1/550$, and the smaller the elastic inter-story drift angle, the stiffer the structure. The definition of the interlayer displacement angle is also realized by the definition of the horizontal displacement. To reduce excessive horizontal displacement, it is often necessary to improve the lateral stiffness of the building. Because excessive horizontal displacement will pose security risks to the structure and affect the comfort of use, it is of great research significance to control the horizontal displacement of the structure.

The floor displacement and interlayer displacement of the models in the X- and Y-directions are shown in Figures 9 and 10. The structure had the maximum interlayer displacement angle on the second floor. This was less than $1/550$, which meets the code requirements. Comparing the interlayer displacement angle in the X-direction and Y-direction, the value in Y-direction was lower. After considering the participation of stairs in the calculation, the maximum interlayer displacement angle in two directions decreased significantly, which indicates that the addition of stairs improves the lateral stiffness of the structure. A comparison of model E and model F found that the interlayer displacement angle of model F was significantly larger than model E, indicating that the lateral stiffness will be reduced after the adoption of the sliding bearing.

(2) Maximum base shear

The comparison of the base shear of each model under the X- and Y-direction earthquake is shown in Figure 11. In Figure 11, the base shear in two directions of model D was relatively close, and the base shear in the Y-direction of both model E and model F was greater than the base shear in the X-direction. The base shear of model E was larger than model D, which indicates that after considering the staircase, the seismic force on the structure increased due to the bracing effect of the staircase slab, and the Y-direction exceeded 37%. The force difference between model D and the actual model E was obvious, illustrating that following the traditional design approach will substantially underestimate the seismic effect on the structure and exacerbate the damage to the building. Compared to

model E, the base shear of model F was reduced, and the decrease in the Y-direction was more significant.

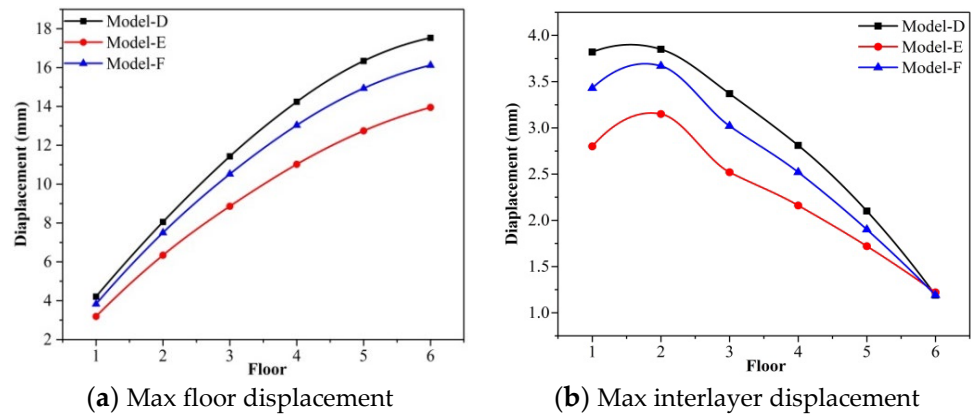


Figure 9. The floor displacement and interlayer displacement in the X-direction.

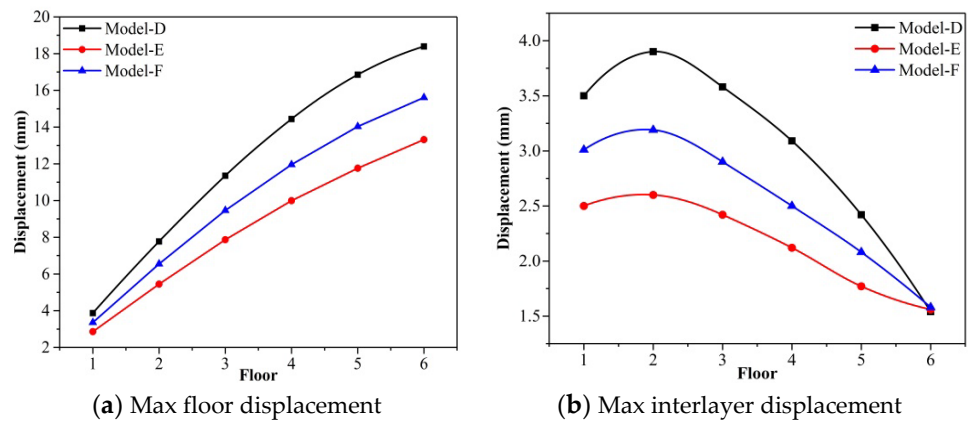


Figure 10. The floor displacement and interlayer displacement in the Y-direction.

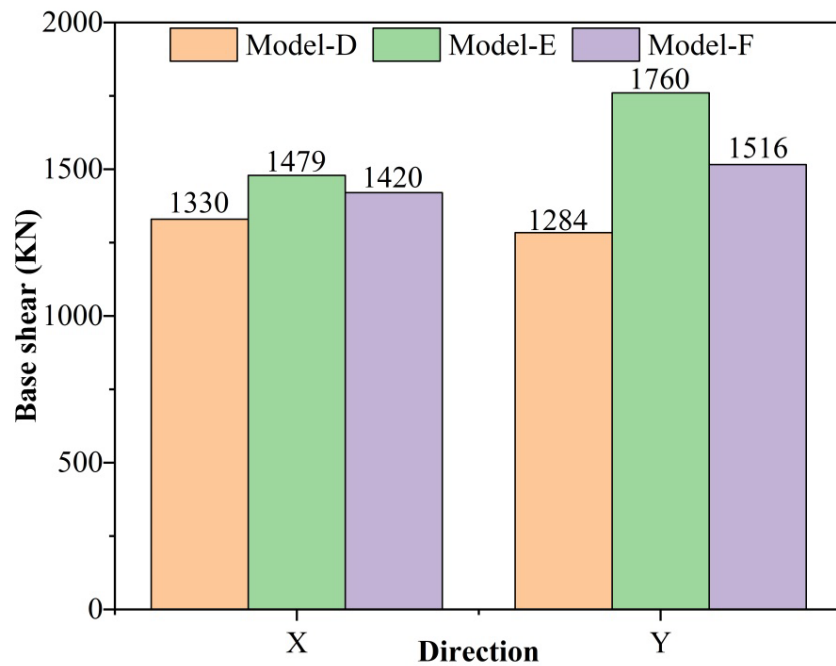


Figure 11. Aa comparison of max base shear of models.

Figure 12 depicts the maximum interlaminar shear forces of each model in the X- and Y-directions. The interlaminar shear force of the bottom was the largest. With the increase in floors, the shear force decreased. Factoring the stairs into the calculation affects the stiffness of the layers; this is more significant on the bottom layer. As the floor height increases, the effect of this impact weakens. The growth rate of model E in the X-direction was 11.2% at the bottom layer and 8% at the top layer. The growth rate of model E in the Y-direction was 37.1% at the bottom and 29.5% at the top. The story stiffness in the Y-direction was found to be more sensitive to the impact of stairs, and the increase was also greater than in the X-direction under the same circumstances. For model F with a sliding connection, the influence will be weaker than in model E, which indicates that the sliding bearing will weaken the seismic response of the building.

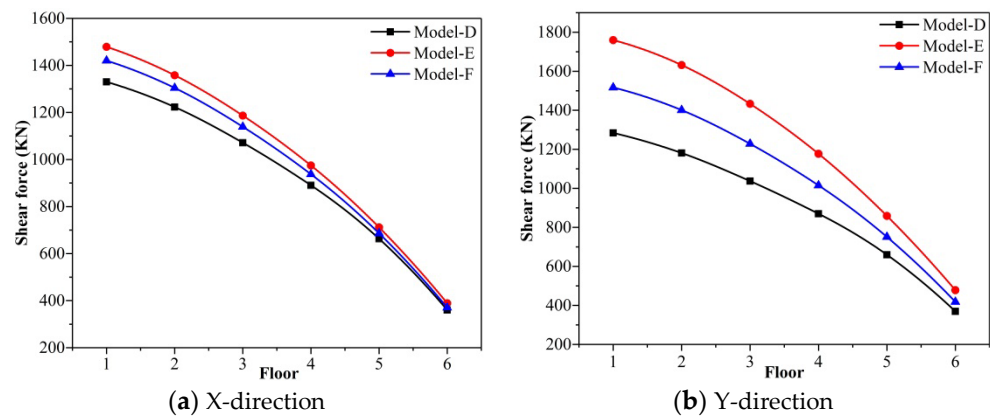


Figure 12. A comparison of the max interlayer shear forces of the models.

(3) Frame force

The previous section found that when stairs are factored into the calculation of the structure, the stiffness of the building in the Y-direction obviously changes. This section will study the X-direction earthquake action under different internal force distributions based on whether the stairs participate in the structure calculation. This paper only selected the frame columns KZ1 and KZ3 at the opposite corners of the staircase and the frame beams KL1–KL4 for comparative analysis. The comparison of internal forces of the beam-column components in different models under the X-direction earthquake is shown in Tables 3–5.

Table 3. Model D.

Components	Internal Force	Floor					
		1	2	3	4	5	6
KL1	Shear force (kN)	17.5	14.6	11.0	6.9	5.3	1.2
	Bending moment (kN·m)	36.8	32.5	25.5	18.6	12.2	4.5
KL2	Shear force (kN)	9.40	8.80	8.00	7.40	6.0	5.1
	Bending moment (kN·m)	13.0	11.5	11.2	9.70	8.9	6.5
KL3	Shear force (kN)	19.7	15.9	12.1	8.10	6.4	2.9
	Bending moment (kN·m)	22.4	18.2	13.4	10.4	8.5	6.5
KL4	Shear force (kN)	14.0	13.4	11.2	9.70	8.6	7.9
	Bending moment (kN·m)	15.8	13.6	11.4	10.6	9.7	7.2
KZ1	Axial force (kN)	54.7	32.4	22.5	15.9	10.5	6.4
	Shear force (kN)	28.1	22.4	17.5	12.4	8.4	5.0
	Bending moment (kN·m)	51.3	43.6	35.4	28.5	18.7	11.0
KZ3	Axial force (kN)	112.7	70.5	52.8	38.2	20.3	12.5
	Shear force (kN)	15.5	14.0	12.5	10.7	8.1	5.1
	Bending moment (kN·m)	32.4	30.0	26.4	20.4	15.2	9.4

Table 4. Model E.

Components	Internal Force	Floor					
		1	2	3	4	5	6
KL1	Shear force (kN)	18.2	16.8	13.1	9.3	6.8	1.7
	Bending moment (kN·m)	42.9	39.4	30.7	21.7	15.7	6.2
KL2	Shear force (kN)	28.0	23.5	18.5	14.6	8.4	6.8
	Bending moment (kN·m)	34.4	29.1	23.0	16.0	12.5	6.6
KL3	Shear force (kN)	21.7	18.4	14.3	10.9	8.2	4.1
	Bending moment (kN·m)	27.5	22.0	16.5	13.2	10.8	8.4
KL4	Shear force (kN)	59.2	53.2	42.9	25.0	18.7	8.7
	Bending moment (kN·m)	75.5	70.0	57.3	37.9	22.7	10.2
KZ1	Axial force (kN)	132	87.9	51.1	32.9	25.2	16.9
	Shear force (kN)	55.1	41.2	32.1	25.0	15.7	10.5
	Bending moment (kN·m)	74.4	54.5	48.0	41.0	33.8	21.6
KZ3	Axial force (kN)	188.2	120.1	80.5	51.1	32.5	22.5
	Shear force (kN)	21.1	19.4	17.4	15.1	12.1	8.1
	Bending moment (kN·m)	47.0	45.7	38.2	31.3	25.3	13.7

Table 5. Model F.

Components	Internal Force	Floor					
		1	2	3	4	5	6
KL1	Shear force (kN)	26.2	22.1	18.7	14.1	9.1	2.5
	Bending moment (kN·m)	52.5	45.2	38.5	30.1	22.0	13.4
KL2	Shear force (kN)	35.1	30.2	23.4	16.8	10.9	7.0
	Bending moment (kN·m)	41.2	35.6	26.8	20.6	16.3	9.5
KL3	Shear force (kN)	26.9	24.3	19.4	16.2	13.2	7.5
	Bending moment (kN·m)	34.6	29.4	25.7	20.4	15.1	12.0
KL4	Shear force (kN)	66.2	60.1	52.1	32.5	24.9	8.4
	Bending moment (kN·m)	85.4	75.8	61.2	45.8	23.0	11.5
KZ1	Axial force (kN)	68.3	46.7	31.5	24.8	18.4	9.8
	Shear force (kN)	40.5	32.4	23.6	15.7	10.8	8.5
	Bending moment (kN·m)	62.5	45.3	41.2	34.2	22.5	11.3
KZ3	Axial force (kN)	157	90.8	61.6	44.1	19.9	10.3
	Shear force (kN)	18.9	18.0	16.5	14.1	11.0	6.4
	Bending moment (kN·m)	42.1	38.4	31.2	25.4	18.4	10.8

The changing trend of KL1's shear force and bending moment with the number of floors was the same. The internal force value of model E was slightly larger than that of model D. The maximum difference was the bending moment of the second floor, with a difference of 21.2%, and the minimum difference was the shear force of the first floor, with a difference of 4.0%. The internal force value of model F was larger than model D; the largest difference was the fourth-floor shear force, the difference was more than one time, and the smallest difference was the sixth-floor shear force.

For KL2: Unlike KL1, the internal force of model D did not decrease much with the number of floors. From the bottom to the top floor, the shear force and bending moment decreased by 45.7% and 50%, respectively. The internal forces of KL2 in model E and model F were similar to those in KL1. The internal forces of the three models decreased as the number of layers increased, and the decrease ratio of model D was the smallest, within 10%, and the decrease rate of the other two models was larger, more than 20% for each layer. The shear force of model F in the first layer was more than three times that of model D.

With the increase in the number of layers, the gap gradually closed, and the change in the bending moment value was similar to the shear force.

For KL3, the changing trend in the shear force and bending moment was the same as KL1. The order of internal force values from largest to smallest was model F > model E > model D, and the decrease rate of the three models was similar. For KL4, the changing trend of internal force was similar to KL2, the decrease in model F and model E was significantly greater than model D, and the internal force value of the model F was not much different from model D.

For KZ1, the internal force also decreased as the number of layers increased, and the feature was model E > model F > model D. The axial force of the first layer increased from 51.3 kN of model D to 132 kN of model E, with an increase of 157.3%. The shear force increased from 28.1 kN to 55.1 kN, with an increase of 96.1%, and the bending moment increased from 51.3 kN·m to 71.4 kN·m, with an increase of 39.2%. For KZ3, the changing trend was consistent with KZ1, the difference between model E and model D was the largest, and between model E and model F it was the smallest. The axial force changed from 112.7 kN to 188.2 kN, which increased by 67.0%, and the shear force changed from 14 kN to 19.4 kN, which increased by 38.6%. The bending moment increased from 30 kN·m to 45.7 kN·m, with an increase of 52.3%.

For the frame beams and columns, the internal force values on the top floors of each model did not change because there were no stairs, which indicates that the influence of stairs on the internal force of the structure is focused on the floor that has staircases, and the influence on the floors without stairs is small.

To sum up, the internal forces of the structural components gradually decrease as the number of floors increases, and the presence or absence of stairs has a greater impact on the internal forces of structural members. When there are stairs in the structure, the stiffness of the building will be increased, and it will be able to bear more seismic action. The internal force of the structural components is also significantly greater than that of the structure without stairs. The frame column's internal force of model F was smaller than that of model E. The frame beam's shear force and bending moment are magnified, so the influence should be considered in structural design.

(4) Internal force of components

Changing the connection mode of stairs will have a corresponding impact on the internal force of the staircase frame. It is conceivable that the internal forces of the stair components, which are the components of the stair units, will also change accordingly. In this section, the A-B/2-3 axis staircase (The staircase A in Figure 5a) is used to study the trends in the change in the internal force of the stair beams and stair columns under the X-direction earthquake action.

(a) Stair columns

As the top of the stair column is connected with the stair beam, it is easy for an earthquake to damage the top of the column. Table 6 compares the axial force and shear force of the stair column (SC1 in Figure 5a) at the intersection of the 1/A axis and 2 axis. After the sliding connection bearing was adopted, the axial force and shear force of the stair column are significantly reduced; the shear value of each layer was reduced by more than 50%, and the shear value of the first layer by 73.2%. The shear force of the stair column with the fixed connection was more than 2.5 times that with the sliding connection, which indicates that the sliding bearing can increase the structure's stiffness and mitigate the damage to the column top.

(b) Stair beams

According to the traditional design method, it is difficult for the reinforcement of the stair beam to meet the needs of the complex stress state during an earthquake, which can lead to failure. Table 7 compares the shear force and bending moment of the stair beam at the intersection of axis 1/A and axes 2-3 (The SB1 in Figure 5a). The internal forces of

model F were weaker than those of model E, and the decrease in the shear force was more pronounced, which indicates that the sliding connection can improve the stress state of the stair beam and reduce the damage caused by an earthquake.

Table 6. A comparison of the internal force of the stair columns.

Story	Model E		Model F	
	Axial Force (kN)	Shear Force (kN)	Axial Force (kN)	Shear Force (kN)
5	34.0	4.9	13.9	1.8
4	49.2	7.0	20.0	2.7
3	61.7	8.6	24.0	3.3
2	69.8	9.9	24.3	3.7
1	61.2	9.7	16.4	3.6

Table 7. A comparison of the internal force of stair beams.

Story	Model E		Model F	
	Shear Force (kN)	Bending Moment (kN·m)	Shear Force (kN)	Bending Moment (kN·m)
5	18.3	19.0	3.5	9.6
4	25.0	23.7	4.7	12.8
3	33.2	34.2	6.0	16.4
2	36.4	41.5	7.2	20.0
1	31.5	37.4	6.2	19.3

4.1.3. Time History Analysis

When using ETABS for the time history analysis, factors such as the site type of the model, the fortification intensity, and the principle of seismic wave selection, the Coalinga wave (T1), Whittier–Narrows wave (T2), and an artificial wave (T3) were selected, respectively. The duration of the three seismic waves was 40 s. Three seismic waves were input horizontally and bidirectionally, and the nonlinear dynamic response of the structure was analyzed under the seismic fortification intensity of six degrees. After checking, it can be seen that the shear force at the bottom of the building obtained under the three seismic waves met the requirements of the specification. The time–history curve of each seismic wave is shown in Figure 13.

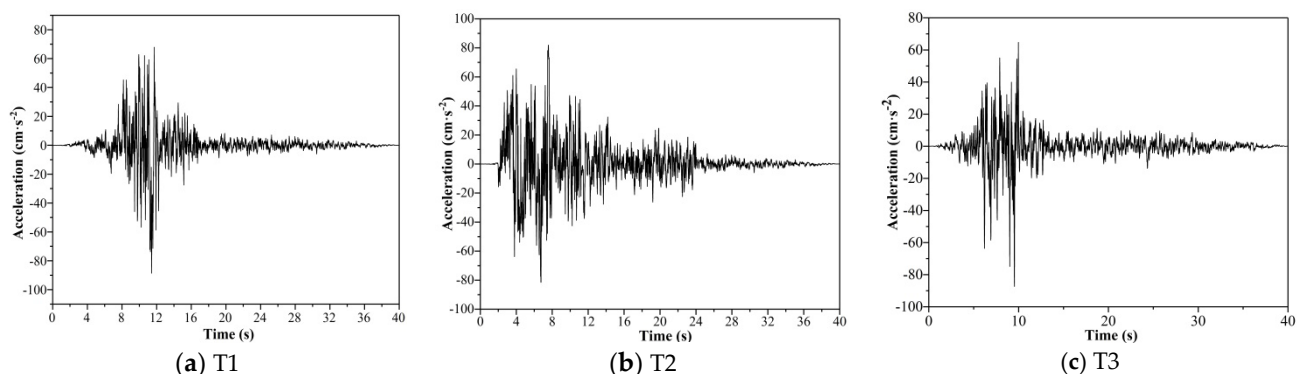


Figure 13. The time-history curves of the seismic waves.

(1) Maximum base shear

Tables 8 and 9 depict the maximum base shear force and corresponding time of the model under the action of each seismic wave. Figure 14 shows the maximum base shear of each model in the X- and Y-directions under each seismic wave.

Table 8. The maximum base shear in the X-direction.

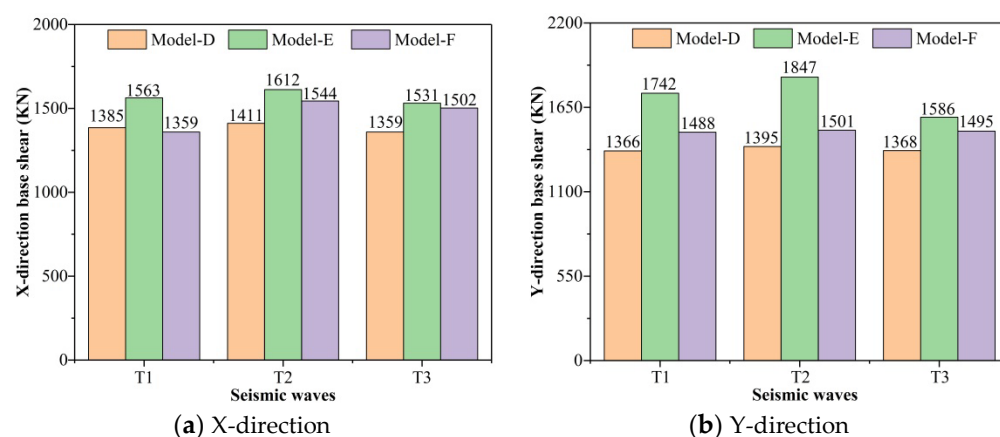
Models	T1		T2		T3	
	MBS (kN)	Time (s)	MBS (kN)	Time (s)	MBS (kN)	Time (s)
Model D	1385	9.22	1411	6.36	1359	4.58
Model E	1563	8.94	1612	6.12	1531	5.14
Model F	1359	9.30	1544	6.22	1502	5.26

Table 9. The maximum base shear in the Y-direction.

Models	T1		T2		T3	
	MBS (kN)	Time (s)	MBS (kN)	Time (s)	MBS (kN)	Time (s)
Model D	1366	8.86	1395	6.30	1368	4.86
Model E	1742	9.08	1847	6.22	1586	4.92
Model F	1488	9.14	1501	6.32	1495	5.12

Note: MBS is the maximum base shear.

The maximum base shear of the three models was 1395 kN, 1847 kN, and 1501 kN. Under the three seismic waves, the three models showed similar trends. The seismic response under T2 was the largest, so different seismic waves will produce different seismic actions, with different impacts on the structure. Under the same seismic wave, each model had a different seismic response. The seismic response of model E was the largest, similar to the results of the response spectrum analysis. The results showed that considering the role of stairs in the seismic analysis will increase the base shear of the structure. Compared to the fixed connection, the sliding bearing can reduce the seismic response of the stairs, increase the energy dissipation capacity of the building, and improve the seismic performance of the frame structure.

**Figure 14.** A comparison of the max base shear of the models.

(2) Maximum vertex displacement

The maximum vertex displacement and corresponding time of each model under the action of each seismic wave were sorted and counted as shown in Tables 10 and 11. The comparison of vertex displacement of each model in the X- and Y-directions is shown in Figure 15.

The maximum vertex displacements of the same model under the action of three seismic waves were not different, and can be arranged in order as $T2 > T3 > T1$. The seismic response of the same seismic wave on different structures was also different, and the trend of the three models was similar. Under the T2 seismic wave, the vertex displacement of model D was the largest among the three models, and the maximum in the Y-direction was 19.13 mm. Under the T3 seismic wave, the vertex displacement of model E was the smallest,

and the minimum value was 14.26 mm in the X-direction. The results show that the fixed connection can effectively reduce the maximum vertex displacement of the structure and increase the structural integrity.

Table 10. The maximum vertex displacement in the X-direction.

Models	T1		T2		T3	
	MVD (mm)	Time (s)	MVD (mm)	Time (s)	MVD (mm)	Time (s)
Model D	17.95	8.62	18.11	6.02	17.82	5.10
Model E	14.32	9.18	14.53	6.18	14.26	4.96
Model F	16.38	8.94	16.87	6.24	16.55	5.04

Table 11. The maximum vertex displacement in the Y-direction.

Models	T1		T2		T3	
	MVD (mm)	Time (s)	MVD (mm)	Time (s)	MVD (mm)	Time (s)
Model D	18.69	8.84	19.13	6.10	19.05	5.08
Model E	14.52	8.76	15.21	6.14	14.85	5.16
Model F	16.22	9.16	15.97	6.22	16.14	4.94

Note: MVD is the maximum vertex displacement.

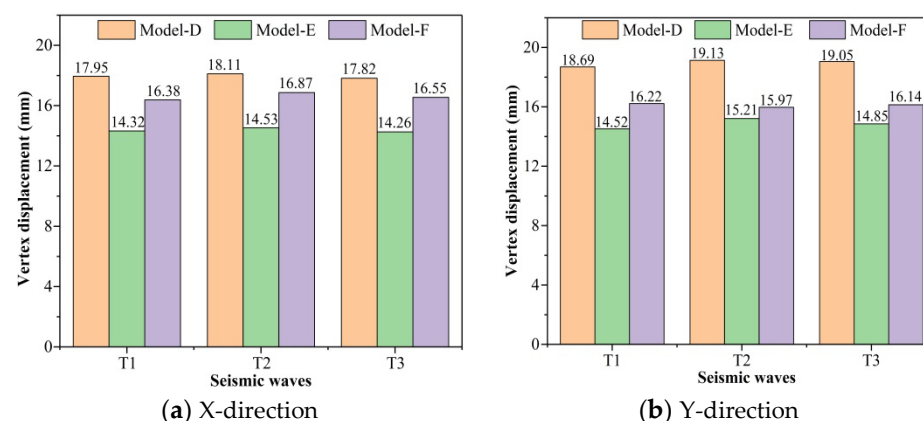


Figure 15. The maximum vertex displacement comparisons of the models.

(3) Maximum interlayer displacement

The maximum interlayer displacement and corresponding time of each model under the action of each seismic wave are listed in Tables 12 and 13. The comparison of the maximum interlayer displacement of each model in the X- and Y-directions is shown in Figure 16.

Table 12. The maximum interlayer displacement in the X-direction.

Models	T1		T2		T3	
	MID (mm)	Time (s)	MID (mm)	Time (s)	MID (mm)	Time (s)
Model D	3.98	8.96	4.12	6.20	4.09	5.04
Model E	3.35	9.08	3.53	6.08	3.50	5.12
Model F	3.62	9.14	3.85	6.26	3.72	4.98

Under the action of each seismic wave, the maximum interlayer displacement in the X- and Y-directions of the three models was close to the results obtained by the response spectrum analysis, and the difference was less than 10%. On the whole, the results are consistent with the response spectrum analysis, which verifies the reliability of the time

history analysis method and can act as a reference for structural seismic performance analysis. The displacement of the T3 wave was closer to the results of response spectrum analysis than the other two waves. The maximum interlayer displacement of different structures appeared at different times under the same seismic wave, so it is necessary to select the appropriate seismic wave according to the actual situation of the building site to obtain more accurate data.

Table 13. The maximum interlayer displacement in the Y-direction.

Models	T1		T2		T3	
	MID (mm)	Time (s)	MID (mm)	Time (s)	MID (mm)	Time (s)
Model D	4.14	9.10	4.25	6.22	4.21	4.92
Model E	3.05	9.02	3.36	6.14	3.24	4.98
Model F	3.11	9.18	3.52	6.08	3.36	5.04

Note: MID is the maximum interlayer displacement.

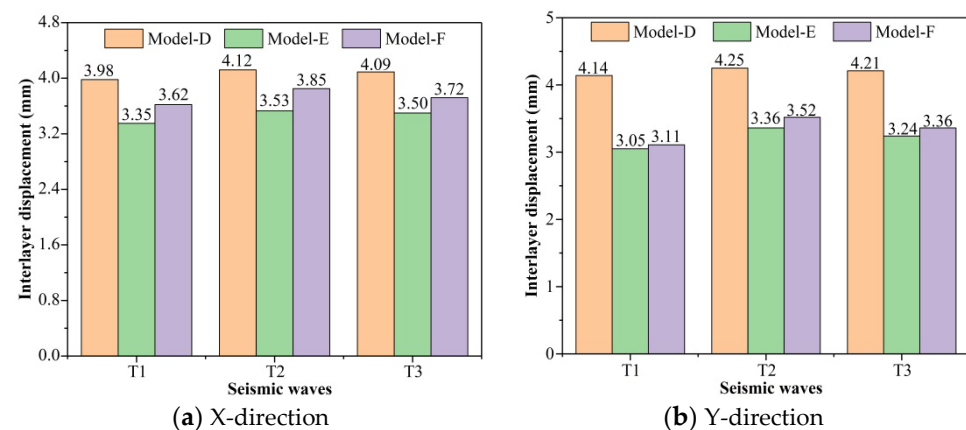


Figure 16. A comparison of the maximum interlayer displacement of the models.

4.2. Different Staircase Positions

4.2.1. Modal Contrast

The first 12 vibration modes of each model structure were extracted, and the natural period of each model was compared (Figure 17). The vibration mode direction is shown in Table 14. In Figure 17, the natural periods of the first three vibration modes of model G were slightly larger than in the other two models. The natural periods of the three models were close, indicating that changing the position of the stairs had little effect on the natural period.

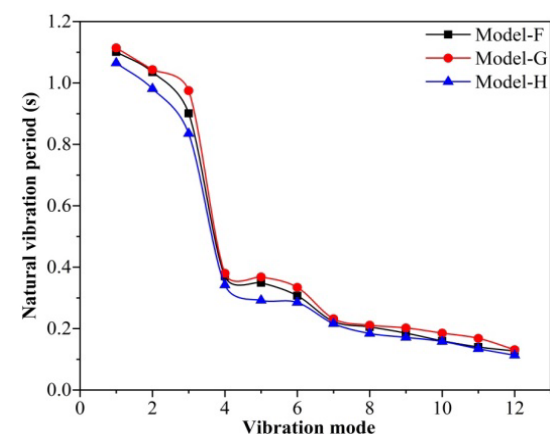


Figure 17. Comparison of natural vibration period.

In Table 14, the first three vibration mode directions of the three models were translation in the X- and Y-directions, and torsion in the Z-direction. Compared with the mass

participation coefficient of each model, although the second mode of model F and model H was Y-direction translation, there was also a part of Z-direction torsion, accounting for 15.2% and 8.6%, respectively. The second mode of model G was not torsional. Compared to the third mode shape of each model, it was a torsional mode shape and the natural vibration period of each model was quite different: the difference between model G and model F was 7.6%, and between model G and model H, it was 14.4%. There was little difference in the translational stiffness of each model, and this difference was mainly reflected in the torsional stiffness.

Table 14. The direction of the first three modes of the models.

Vibration Model	Model F	Model G	Model H
1	X-translation	X-translation	X-translation
2	Y-translation	Y-translation	Y-translation
3	Z-torsion	Z-torsion	Z-torsion

4.2.2. Response Spectrum Analysis and Contrast

(1) Maximum horizontal displacement contrast

Figure 18 compares the maximum interlayer displacement of the model under the action of an earthquake. Under the action of a horizontal earthquake, the total X-direction displacement is as follows: model H > model G > model F, the maximum difference was 1.7 mm, and the difference was 11.8%. The maximum story displacement of each model in the X-direction occurred in the second story. According to the order of model H, model G, and model F, the story displacement of the second story was 3.67 mm, 3.42 mm, and 3.08 mm, respectively. The interlayer displacement angles of the second story were 1/995, 1/1140, and 1/1266, respectively, all less than 1/550, and met the specification. The results show that changing the location of stairs had little effect on the horizontal displacement of the structure.

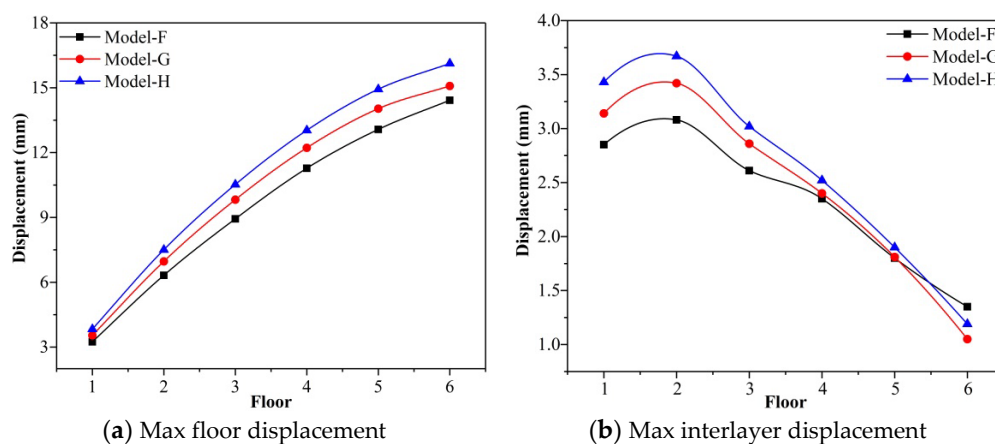


Figure 18. The floor displacement and interlayer displacement in the X-direction.

Under the horizontal earthquake action in the Y-direction, the max floor displacements of the models in the Y-direction were 15.61 mm, 14.53 mm, and 13.68 mm, respectively (Figure 19). Model H was 7.4% larger than model G and 14.4% larger than model F. The maximum interlayer displacement in the Y-direction also appeared in the second layer, model H was 3.19 mm, and the interlayer displacement angle was 1/1231. Model G was 2.95 mm, and the interlayer displacement angle was 1/1322. The model F was 2.85 mm, and the inter-story drift angle was 1/1368, which was less than 1/550 and met the requirements of the code. The results showed that the maximum interlayer displacement of model H in the Y-direction was greater than that of model G under horizontal seismic action. This indicates that the lateral stiffness of the structure will be reduced when the stairs are symmetrically arranged.

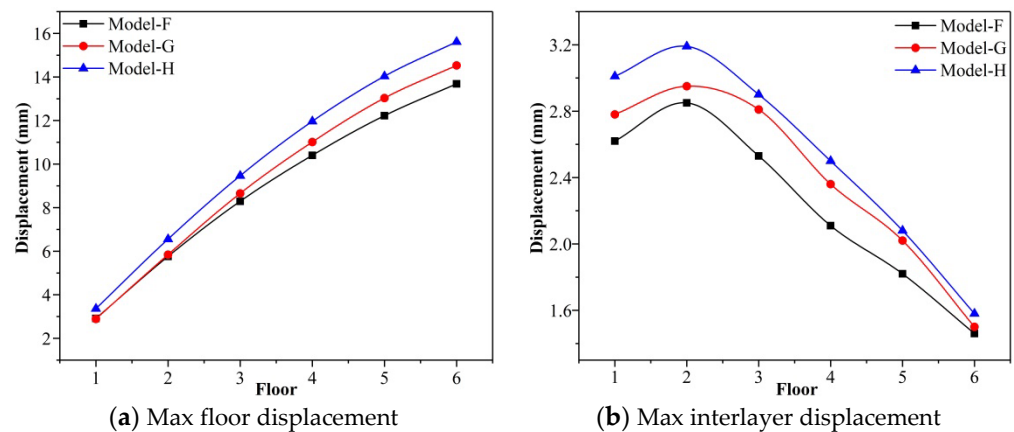


Figure 19. The floor displacement and interlayer displacement in the Y-direction.

The total horizontal displacement variation of the three models in the X- and Y-directions was basically the same, and the interlayer displacement variation of each model was also similar. The maximum horizontal displacement and the maximum inter-story displacement of model H were the largest among the three models, and model F was the smallest among the three models. The horizontal displacement change rate in the Y-direction was larger than in the X-direction. It shows that changing the location of the stairs will affect the horizontal displacement of the structure, and the Y-direction has a slightly significant impact.

(2) Maximum base shear contrast

The calculation results of the maximum base shear of different models under the X- and Y-direction seismic action are in Table 15. The calculation results of each model were compared with those of model F to analyze the influence of the change in the staircase position on base shear under seismic action. The base shear in the X-direction was less affected by the staircase position. The largest difference was between model H and model F, with a difference of 5.4%. The gap in the Y-direction was more pronounced, and that in model G and model H was larger than model F by 5.5% and 13.3%, respectively. The shear force in the Y-direction was larger than in the X-direction. This shows that changing the staircase location will affect the seismic action of the structure, and the shear force of the structure will be increased if the stairs are arranged to the outside span or in a central symmetrical way, and the effect of the latter is more pronounced.

Table 15. A comparison of the maximum base shear of the models.

Models	X-Direction		Y-Direction	
	Shear Force (kN)	Change Rate	Shear Force (kN)	Change Rate
F	1420	–	1516	–
G	1395	1.8%	1432	5.5%
H	1344	5.4%	1315	13.3%

(3) Frame force contrast

In this section, we will study the internal force change of the whole frame after changing the position of the stairs under the earthquake action in the X-direction. The frame columns KZ1 and KZ3 and the frame beams KL1–KL4 were selected for comparative analysis (as shown in Figure 6). The internal force comparison of each component of model G and model H under the X-direction seismic action is shown in Tables 16 and 17.

Table 16. Model G.

Components	Internal Force	Floor					
		1	2	3	4	5	6
KL1	Shear force (kN)	22.4	20.1	15.9	12.1	7.0	2.1
	Bending moment (kN·m)	49.7	43.6	33.4	25.4	15.7	12.1
KL2	Shear force (kN)	33.1	30.4	25.4	16.5	10.1	8.0
	Bending moment (kN·m)	38.9	33.2	25.4	18.5	14.5	8.1
KL3	Shear force (kN)	22.5	19.2	16.4	13.0	10.4	6.1
	Bending moment (kN·m)	30.1	28.9	26.2	18.4	11.1	9.2
KL4	Shear force (kN)	54.2	45.1	40.3	30.5	24.6	11.7
	Bending moment (kN·m)	68.2	60.1	52.7	44.8	31.6	17.5
KZ1	Axial force (kN)	124.3	100.7	75.1	51.9	29.4	12.5
	Shear force (kN)	65.8	51.7	39.4	25.6	18.7	11.8
	Bending moment (kN·m)	88.7	76.3	62.4	45.1	24.5	15.4
KZ3	Axial force (kN)	184.5	156.2	116.1	71.5	43.8	20.4
	Shear force (kN)	45.7	37.8	28.5	20.5	14.1	8.1
	Bending moment (kN·m)	60.3	42.6	42.6	31.1	22.6	10.4

Table 17. Model H.

Components	Internal Force	Floor					
		1	2	3	4	5	6
KL1	Shear force (kN)	20.3	17.8	13.6	10.5	6.8	2.0
	Bending moment (kN·m)	43.5	38.7	29.7	20.1	14.3	11.2
KL2	Shear force (kN)	31.0	29.5	23.5	14.8	8.4	7.5
	Bending moment (kN·m)	35.4	31.0	24.3	16.0	10.6	7.5
KL3	Shear force (kN)	21.4	17.4	13.3	10.4	7.7	5.2
	Bending moment (kN·m)	28.2	26.4	22.1	14.8	10.5	8.6
KL4	Shear force (kN)	47.2	40.1	34.8	25.9	18.5	10.1
	Bending moment (kN·m)	58.7	52.4	45.7	37.6	25.8	14.3
KZ1	Axial force (kN)	66.7	50.8	30.7	22.5	15.2	9.0
	Shear force (kN)	38.9	31.7	24.2	15.1	10.0	8.60
	Bending moment (kN·m)	60.4	43.1	38.4	32.5	22.7	10.3
KZ3	Axial force (kN)	108	85.1	65.2	42.1	15.5	10.0
	Shear force (kN)	18.3	17.5	16.6	13.5	11.4	6.20
	Bending moment (kN·m)	41.2	39.4	31.5	24.8	17.4	10.4

The shear force and bending moment of KL1 decreased as the number of floors increased, and the changing trends of the three models were not different. The maximum internal force was in model F, followed by model G, and the smallest was in model H. The difference in shear force between model F and model H on the first floor was 5.9 kN, and the bending moment was 9 kN·m. Except for a few layers, the difference between the internal forces became smaller and smaller as the number of floors increased. On the top floor, the internal forces of the three models were similar.

The internal force of KL2, KL3, and KL4 was similar to KL1, and KL4 was the biggest. When the position of the stairs is changed, the change ratio of the internal force of KL2 was smallest, the change in the shear force was less than 5 kN, and the change in the bending moment was 5.8 kN·m. The internal force of KL3 showed a larger change. For KL4, based on model F, the internal force level was relatively close when the stairs were centrally symmetrical and placed at the side span, and the internal force was slightly larger when placed at the side span. The internal force of KL4 in model F was still the largest among the three models, the shear force had a significant decline on the fourth floor, and the decline

rate reached 37.6%. The bending moment values of the fifth and sixth floors were slightly smaller than model G and model H.

For KZ1, the internal force of model G was much larger than the other two models, and model F and model H were very close. In model G, the maximum axial force was 124.3 kN on the first floor, while in model F, the axial force was 68.3 kN, and model H was 66.7 kN, model G was 1.82 times that of model F. The maximum values of the shear force and bending moment in model G were 65.8 kN and 88.7 kN·m, respectively, more than 1.4 times the other two models. For KZ3, the axial force of the first layer of model F was 157 kN, which was not significantly different from the 184.5 kN of model G. The axial force of model F was very close to model H from the second layer, which was lower than model G. The change in the shear force and bending moment of KZ3 was similar to KZ1. The internal force of model G was the largest, and the internal force of model F and model H was similar and smaller.

To sum up, changing the position of the staircases will affect the internal force distribution of the structure. When the stairs are at the side span, the internal force of the frame columns will increase significantly, but the frame beams will not. When the position of the stairs is centrosymmetric, the internal forces of the frame beams and columns are relatively lower.

(4) Comparison of internal forces of stair components

(a) Ladder columns

Table 18 shows the internal forces of ladder column SC2 in model G and SC3 in model H. The axial forces of the second layer of each model are as follows: model F—24.3 kN (Table 6), model G—25.4 kN, and model H—23.1 kN. The axial force of the stair column of model G was the largest, and that of model H was the smallest. The shear force of the stair column on the second floor of each model was 3.7 kN for model F, 4.2 kN for model G, and 3.7 kN for model H. The shear force of the stair column on model G was the largest, and the shear force on model F was the same as that of model H. This indicates that the axial and shear force on the stair columns will decrease after the stairs are centrally symmetrical design. When the stairs are at the side span, the internal force of the stair columns will increase.

Table 18. A comparison of the internal force of the ladder columns.

Stories	Model G		Model H	
	Axial Force (kN)	Shear Force (kN)	Axial Force (kN)	Shear Force (kN)
5	13.6	2.1	14.2	1.8
4	20.5	2.7	19.4	2.4
3	23.1	3.4	23.0	3.1
2	25.4	4.2	23.1	3.7
1	16.7	3.9	15.6	3.2

(b) Ladder beams

Table 19 shows the internal forces of ladder beam SB2 in model G and SB3 in model H. The shear force of model F was 7.2 kN, and the bending moment was 20.0 kN·m; the shear force of model G was 8.0 kN, and the bending moment was 23.8 kN·m; the shear force and bending moment of model H were 6.5 kN and 18.5 kN·m, respectively. Compared with model F, the shear force of each layer in model G increased by about 10%, and the bending moment of each layer increased by more than 15%. The internal force change in the stair beams under different stair positions showed that placing the staircases at the side span is not conducive to reducing the component damage caused by earthquake.

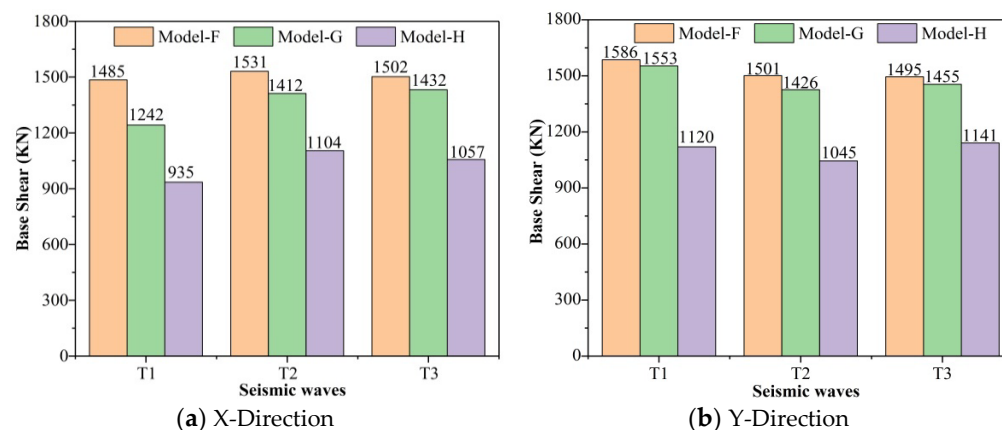
Table 19. A comparison of the internal force of the ladder beams.

Stories	Model G		Model H	
	Shear Force (kN)	Bending Moment (kN·m)	Shear Force (kN)	Bending Moment (kN·m)
5	4.1	11.2	3.0	9.4
4	5.4	15.1	4.3	11.9
3	7.5	19.4	6.2	16.2
2	8.0	23.8	6.5	18.5
1	7.1	22.5	5.8	17.2

4.2.3. Time History Analysis and Contrast

(1) Maximum base shear contrast

Figure 20 shows the maximum base shear of each model in the X- and Y-directions. The max base shear of the models was different under different seismic waves. Under the same seismic wave, the seismic response of model F was the largest and that in model H the smallest. Under the T2 seismic wave, the max base shear of model F was 1531 kN, and that of model H was 1104 kN. It appeared early under the T3 seismic wave and late under the T1 seismic wave. Under different seismic waves, all maximum base shears of model H were the smallest, which shows that the stairs placed on the side span reduce the seismic response of the structure.

**Figure 20.** The maximum base shear of the models.

(2) Maximum vertex displacement contrast

Figure 21 lists the maximum vertex displacement of each model in the X- and Y-directions under the action of different seismic waves. It can be seen from the figure that there were no features for the change in the vertex displacement under three seismic waves. For the same model, the vertex displacement produced by each seismic wave did not differ. Under the same seismic wave, the vertex displacement of model H was the largest among the three models, and the maximum was 17.25 mm under the T3 seismic wave. The vertex displacement of model F was the smallest, and the minimum value was the displacement produced by the T1 seismic wave, which was 16.38 mm. The results show that the maximum vertex displacement of the structure is affected by the location of the staircases.

(3) Maximum interlayer displacement contrast

In Figure 22, the maximum interlayer displacement of the three models in the X- and Y-directions was different. The variation trend of the maximum interlayer displacement generated by three seismic waves acting on the same structure was close to the results obtained in the response spectrum analysis. The maximum interlayer displacement of model H was the largest among the three models, and the results obtained under the three

seismic waves were the same. The structure will produce different displacement responses to different seismic waves. Generally speaking, the maximum interlayer displacement of each model under the T2 seismic wave was the largest among the three seismic waves. The results show that the symmetrical design of staircases will reduce the lateral stiffness of the structure.

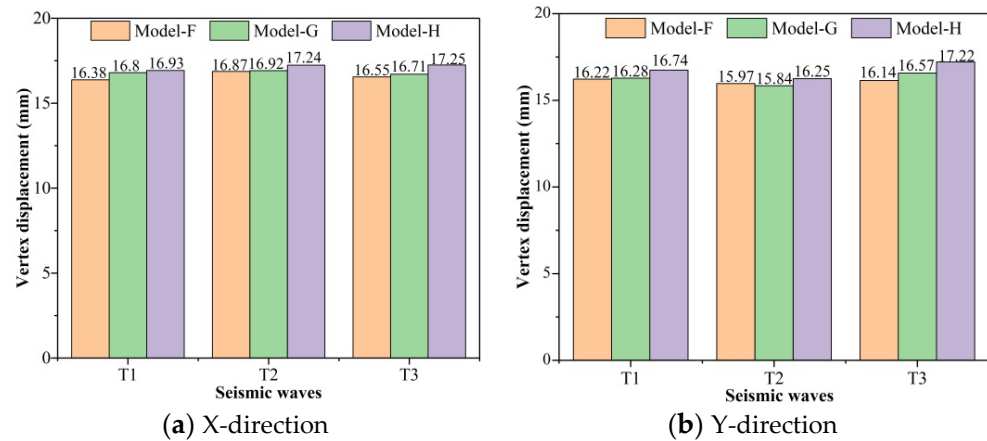


Figure 21. The maximum vertex displacement of the models.

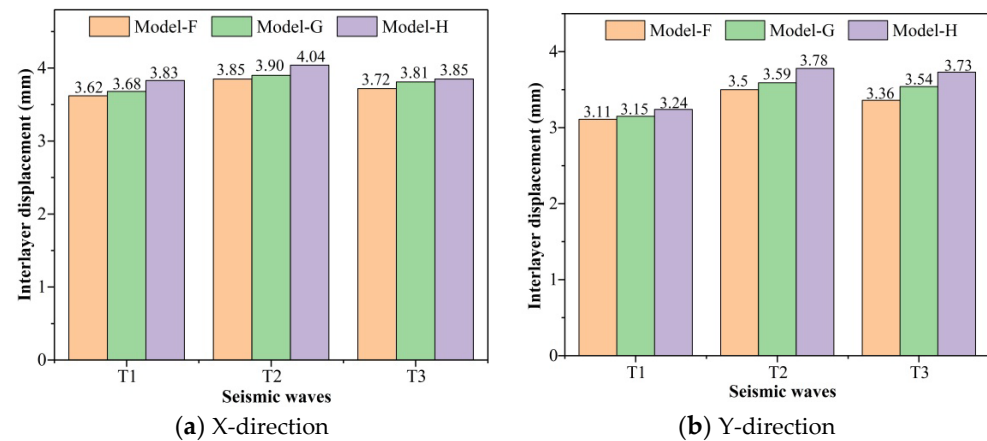


Figure 22. The maximum interlayer displacement of the models.

5. Conclusions

In this paper, a pure frame model without staircases, a frame model with fixed connection beam staircases, and a frame model with sliding connection beam staircases were established by ETABS. According to an engineering example, the modal analysis, response spectrum analysis, and elastic time-history analysis were carried out on each model. The influences of different connection modes of staircases on the structure's seismic performance were studied from the maximum floor displacement, inter-story displacement angle, natural period, shear force, and internal force of the components of each model. The main conclusions are as follows:

(1) The modal analysis showed that the lateral and torsional stiffness of the sliding connection stairs was less than the fixed connection stairs; so the sliding bearing can reduce the deformation constraint between the stair beams and the landing slabs.

(2) The interlayer displacement angle of the sliding connection bearing was significantly greater than the fixed connection bearing, which indicates that the sliding support can reduce the structure's lateral stiffness. The maximum interlayer displacement angles of models under different research conditions were less than 1/550, which met the construction requirements.

(3) The interlaminar shear at the bottom of the structure was the largest and decreased gradually as the number of floors increased. Moreover, the staircases had a significant

impact on the stiffness of the building. On the bottom layer, the influence was more pronounced; as the number of layers increased, the impact effect was gradually reduced.

(4) For the structural members, the internal force gradually decreased as the number of floors increased. When the stairs were factored into the calculation, the stiffness increased, and the internal force of the staircase members was significantly greater than the structure without stairs. The internal force of the frame columns of model F was smaller than that of model E, but the shear force and bending moment of the frame beams were amplified in model F.

(5) The staircase position had little effect on the structure's natural period. Changing the stair position will affect the horizontal displacement of the building, especially in the Y-direction. Different stair arrangements will also affect the internal force distribution of the overall structure; when the staircases are at the side span, the internal force of the frame columns will increase significantly, but the frame beam will not.

This paper examined the seismic performance of beam staircases with different types of bearings, but there are still some shortcomings. In the follow-up study, the energy dissipation effect of beam staircases will be studied by using different energy dissipation devices based on the different types of bearings.

Author Contributions: Conceptualization, M.W.; Data curation, M.W.; Formal analysis, M.W.; Investigation, B.C. and M.W.; Methodology, M.W., B.C. and H.F.; Project administration, B.C.; Resources, W.W.; Software, H.T. and W.W.; Supervision, M.W. and B.C.; Validation, H.T.; Funding acquisition, B.C.; Visualization, H.T.; Writing—original draft, H.T.; Writing—review & editing, H.F. All authors have read and agreed to the published version of the manuscript.

Funding: This work was supported by the National Natural Science Foundation of China (grant number 51868048) and the China Earthquake Administration Basic Research Project (grant number 2018D18). The authors are sincerely grateful for this financial support.

Institutional Review Board Statement: Not applicable.

Informed Consent Statement: Not applicable.

Data Availability Statement: Not applicable.

Conflicts of Interest: We confirm that the manuscript has been read and approved by all of the named authors and that there are no other persons who satisfied the criteria for authorship but are not listed. We further confirm that the order of authors listed in the manuscript has been approved by all of us.

References

1. Li, B.; Mosalam, K.M. Seismic performance of reinforced-concrete stairways during the 2008 Wenchuan earthquake. *J. Perform. Constr. Fac.* **2013**, *27*, 721–730. [[CrossRef](#)]
2. Zhao, Y. Earthquake-resistant statically determinate stairs in buildings. *Pract. Period. Struct. Des. Constr.* **2016**, *21*, 04016010. [[CrossRef](#)]
3. Cosenza, E.; Verderame, G.M.; Zambrano, A. Seismic performance of stairs in the existing reinforced concrete building. In Proceedings of the 14th World Conference on Earthquake Engineering, Beijing, China, 12–17 October 2008.
4. Bilal, A.; Mohammad, Z.; Baqi, A. Effect of Dog-Legged Staircase on the Seismic Response of Hill Buildings. In *Lecture Notes in Civil Engineering*; Springer: Singapore, 2022; pp. 175–183. [[CrossRef](#)]
5. Cong, S.; Zhang, Z.; Zheng, Q.; Xu, Z. Seismic behavior of reinforced concrete frame staircase with separated slab stairs. *Structures* **2021**, *34*, 4284–4296. [[CrossRef](#)]
6. Liu, J.; Shen, H. Pushover analysis of plate stair diagonal brace role release. *Sichuan Build. Sci.* **2013**, *39*, 176–179. (In Chinese)
7. Ma, X. Influence of Different Stair Shapes on Seismic Performance of RC Frame. *J. Water Resour. Archit. Eng.* **2018**, *16*, 224–229. (In Chinese)
8. Wu, Z.; Li, C.; Jiang, S. Component-performance-based seismic assessment of reinforced concrete plate stairs in existing frameworks. *J. Fuzhou Univ.* **2018**, *46*, 109–114. (In Chinese)
9. Fallahi, S.; Alirezaei, M. Response evaluation of stairways in RC frames under earthquake ground motions. *Int. J. Eng. Sci. Res. Technol.* **2014**, *3*, 6077–6082.
10. Ahmad, S. Curved Finite Elements in the Analysis of Solid, Shell and Plate Structures. Doctoral Dissertation, University College of Swansea, Swansea, UK, 1969.

11. Kam, W.Y. *Preliminary Report from the Christchurch 22 Feb 2011 6.3 Mw Earthquake: Pre-1970s RC and RCM Buildings, and Precast Staircase Damage*; University of Canterbury: Christchurch, New Zealand, 2011.
12. Wang, X.; Astroza, R.; Hutchinson, T.C.; Conte, J.P.; Restrepo, J.I. Dynamic characteristics and seismic behavior of prefabricated steel stairs in a full-scale five-story building shake table test program. *Earthq. Eng. Struct. Dyn.* **2015**, *44*, 2507–2527. [[CrossRef](#)]
13. Karaaslan, A.; Avsar, O. Seismic response of substandard RC frame buildings in consideration of staircases. *Earthq. Struct.* **2019**, *17*, 283–295. [[CrossRef](#)]
14. Feng, Y.; Wu, X.; Xiong, Y.; Li, C.; Yang, W. Seismic performance analysis and design suggestion for frame buildings with cast-in-place staircases. *Earthq. Eng. Eng. Vib.* **2013**, *12*, 209–219. [[CrossRef](#)]
15. Khadse, P.; Khedikar, A. Seismic Analysis of High Rise RC Frame Structure with Staircase at Different Location. *Int. J. Eng. Sci.* **2018**, *1*, 5–20.
16. Zhao, J.; Hou, P.C.; Liu, M.; Tu, J.; Gao, Z.Q.; Peng, L.Y. Shaking table test on structural model of concrete frame-staircase with sliding supports. *J. Build. Struct.* **2014**, *35*, 53–59. (In Chinese) [[CrossRef](#)]
17. Ke, C.R.; Wang, H.Q. Study on seismic performance of frame structure with viscous damping staircase. *J. Phys. Conf. Ser.* **2020**, *1676*, 012069. [[CrossRef](#)]
18. Sun, H.; Zhang, A.; Cao, J. Earthquake response analysis for stairs about frame structure. *Eng. Fail. Anal.* **2013**, *33*, 490–496. [[CrossRef](#)]
19. Rao Botsa, S.; Dasgupta, K. Influence of Staircase and Elevator Core Location on the Seismic Capacity of an RC Frame Building. *J. Archit. Eng.* **2017**, *23*, 05017007. [[CrossRef](#)]
20. Ahmed, O.H.; Hazem, A.R.; Shawky, A.A. Seismic Performance of Staircases in the 3D Analysis of RC Building. *Civ. Eng. J.* **2022**, *7*, 114–123. [[CrossRef](#)]
21. Zhao, J.; Hou, P.C.; Liu, M.; Zhu, Y.Y.; Gao, Z.Q.; Peng, L.Y. Experimental study on seismic performance of concrete frame with staircase under quasi-static loading. *J. Build. Struct.* **2014**, *35*, 44–50. (In Chinese) [[CrossRef](#)]
22. Xiao, J.; Yin, B.J.; Cheng, S.G.; Zhao, X.L. Experimental research and finite element analysis on seismic damage for staircases of RC frame structures. *Build. Struct.* **2014**, *44*, 12–16. (In Chinese)
23. Mir, F.U.H.; Rai, D.C. Experimental and parametric investigation of effects of built-in staircases on the dynamics of RC buildings. *Earthq. Eng. Struct. Dyn.* **2020**, *49*, 527–542. [[CrossRef](#)]
24. Delavar, M.A.; Varnosfaderani, M.P.; Bargi, K. Effects of staircase on the seismic performance of reinforced concrete frame buildings considering the position of the staircase. In Proceedings of the International Conference on Contemporary Iran on Civil Engineering Architecture and Urban Development, Tehran, Iran, 16 August 2017.
25. *11 G101-2 [S]*; National Building Standard Design Atlas. China Planning Press: Beijing, China, 2011.
26. Chandra, S.; Singh, B.K.; Tomar, A. Seismic Assessment of RC Structure with and without Lateral Load Resisting Members. In *Recent Advances in Computational and Experimental Mechanics, Vol II*; Springer: Singapore, 2022; pp. 545–555. [[CrossRef](#)]